Full Paper

Lipase-catalyzed Production of (*S*)-Carprofen Enhanced by Hydroxyethyl-#-cyclodextrins: Experiment and Optimization

Xin Yuan, Guangyong Liu, Pan-Liang Zhang, Weifeng Xu, and Ke-Wen Tang

Org. Process Res. Dev., **Just Accepted Manuscript** • DOI: 10.1021/acs.oprd.9b00009 • Publication Date (Web): 03 Apr 2019

Lipase-catalyzed Production of (*S*)-Carprofen Enhanced by Hydroxyethyl-*β*-cyclodextrins: Experiment and Optimization

Xin Yuan, Guangyong Liu, Panliang Zhang*, Weifeng Xu, Kewen Tang*

Department of Chemistry and Chemical Engineering, Hunan Institute of Science and Technology, Yueyang 414006, Hunan, China

Table of Contents graphic

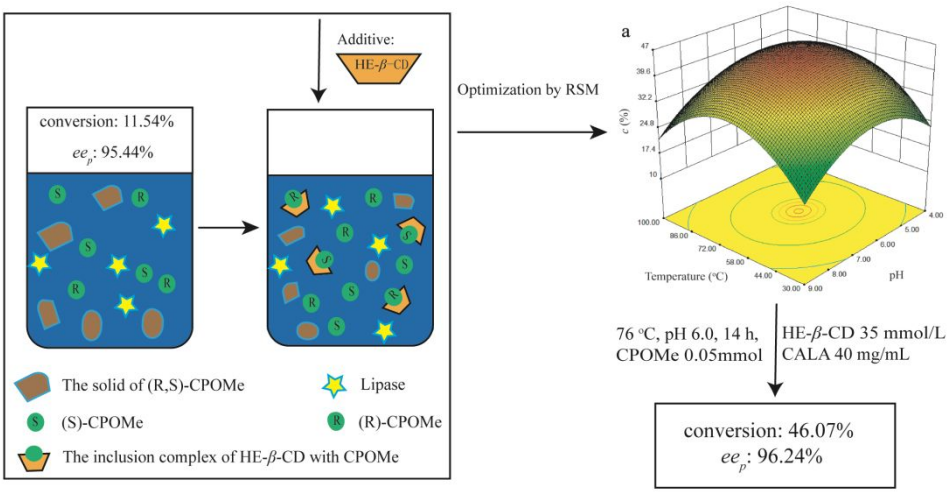

ABSTRACT

Stereoselective resolution of (*R*,*S*)-carprofen methyl ester (CPOMe) by lipase-catalyzed hydrolysis to (*S*)-carprofen (CP) was investigated in an aqueous medium. With the highest catalytic activity, *Candida antarctica* lipase A (CALA) was selected as catalyst compared to eight other lipases. Hydroxyethyl-*β*-cyclodextrin (HE-*β*-CD) was added to enhance the solubility of (*R*,*S*)-CPOMe, which significantly raised the conversion of substrate from 11.12% to 30.84%. Response surface methodology (RSM) was adopted to evaluate the influence of factors on the substrate conversion (*c*) and enantiomeric excess of product (ee_p), such as pH, concentrations of enzyme and HE-*β*-CD, temperature, substrate loading and reaction time. The optimal conditions were obtained, including pH 6.0, 40 mg/mL CALA, 0.05 mmol substrate, 35 mmol/L HE-*β*-CD, agitation speed of 600 rpm, temperature of 76 °C, and reaction time of 30 h. Under above conditions, (*S*)-CP as the desired product was obtained with enantiomeric excess of 96.24% and overall conversion of 46.07%.

Keywords: (*S*)-carprofen; response surface methodology; hydrolysis; hydroxyethyl-*β*-cyclodextrin; Candida antarctica lipase A

INTRODUCTION

The enantiomers of chiral drugs are substantially identical in physical and chemical properties, but they often show significant differences in biological activity[1]. The life system is a chiral environment, so different properties and effects of pharmacological as well as different pharmacokinetic properties will be exhibited with taking racemic drugs[2,3]. On the contrary, optically pure drugs have the advantages of reducing the dose and metabolic burden of the body, which can reduce the risk of side effects caused by the undesired enantiomer[4,5]. Therefore, it is highly preferable to use enantiomerically pure compounds in pharmaceutical field[6].

Generally, methods used to obtain monoenantiotropic drugs are chemical synthesis and racemic resolution. Chemical synthesis is easy to obtain single enantiomer, but the development of this method would be time consuming and expensive[7]. Racemic resolution is simple, easy to industrial production, low cost and short development time[8]. Therefore, it has been dominant in industrial applications. In general, racemic separation techniques include crystallization[9], simulated moving bed chromatography (SMB)[10], membrane[11], enantioselective liquid–liquid extraction (ELLE)[12-14] and so on. However, some disadvantages limit the further development of above methods. For example, chromatography method is low rate of recovery and difficulty in scale-up[15]. Membrane separation method is poor stability and low transport rate[16]. The enzymatic kinetic resolution has been an interesting method[17-23] with its high stereoselectivity and regioselectivity. It may avoid some problems such as producing a large number of ineffective or even harmful enantiomers to the environment caused by chemical synthesis. Enzyme-catalyzed kinetic resolution can be carried out by esterification[17,18], transesterification[19,20], hydrolysis[21-23], etc.

Carprofen (CP, 6-chloro-α-methyl-carbazole-2-acetic acid) is an important non-steroidal anti-inflammatory possessing antipyretic and analgesic effects, which is often used to treat rheumatoid arthritis, rheumatic spondylitis, postpartum postoperative pain and other diseases[5]. The activity of (*S*)-enantiomer is higher 28-fold than the corresponding (*R*)-enantiomer[24]. Therefore, obtaining the optically pure (*S*)-CP is of great significance. At present, several methods to obtain carprofen enantiomers have been reported in the literature, including high performance liquid chromatography[25] and asymmetric hydrogenation[26,27].

In this paper, enzymatic hydrolysis was employed for resolution of (*R*,*S*)-carprofen methyl ester to obtain (*S*)-CP in an aqueous system. However, the solubility of (*R,S*)-CPOMe in aqueous solution was very poor, which resulted in low enzymatic reaction rate and low conversion rate of substrate[28,29]. Herein, adding β-cyclodextrin derivatives to enhance the solubility of (*R,S*)-CPOMe and the hydrolysis reaction rate. The effects of influencing factors had been investigated, including pH, concentrations of enzyme and HE-*β*-CD, temperature, substrate loading, reaction time and so on. To achieve the optimal separation effects, response surface methodology (RSM) was applied to optimize reaction conditions.

EXPERIMENTAL

Materials

Lipase AK "Amano", lipase PS and lipase AY were obtained from Amano pharmaceutical Co., Ltd. (Nagoya, Japan). Novozym 435, *Candida antarctica* Lipase A (CALA), Novozym40086, lipozyme RM IM and lipozyme TL IM were purchased from Novozymes Biopharma DK A/S (Denmark). PPL was purchased from Sigma-Aldrich (USA). (*R*,*S*)-CP was obtained from Xianju Pharmaceutical Co., Ltd. (Zhejiang, China). Hydroxyethyl-*β*-cyclodextrin (HE-*β*-CD) and

Hydroxypropyl-*β*-cyclodextrin (HP-*β*-CD) were purchased from Shandong New Fine Chemical Co., Ltd. (Shandong, China). Methylated-*β*-cyclodextrin (Me-*β*-CD), Sulfobutylether-*β*-cyclodextrin (SBE-*β*-CD) and Carboxymethyl-*β*-cyclodextrin (CM-*β*-CD) were purchased from Shandong Zhiyuan Biotechnology Co., Ltd. (Shandong, China). (*R*,*S*)-CPOMe was prepared in the laboratory. Methanol and acetonitrile were chromatographic grades. Other reagents were analytical grade and supplied by different commercial company.

Aalytical Methods

The concentrations of (*R*,*S*)-CP enantiomers were analyzed on ODS-2 column (150 mm × 4.6mm i.d., 5μm) by HPLC (waters e2695, Waters Corporation, USA) at a wavelength of 273 nm. The mobile phase was composed of methanol and aqueous solution (containing 20 mmol/L sodium dihydrogen phosphate and 25 mmol/L HP-*β*-CD) at the ratio of 35:65 (v/v) (pH = 5.50, adjusted with sodium hydroxide). The column temperature was maintained at 37 °C. The flow rate was kept at 1 mL/min. The injection volume was 10 μL. The retention time of (*R*)-CP and (*S*)-CP were 53.7 min and 60.5 min, respectively. This analytical method was learned from the literature[25].

The enantiomeric excess (ee_p) express the purity of (*S*)-CP in Eq. (1).

$$ee_P = \frac{[S]-[R]}{[S]+[R]} \times 100\% \quad (1)$$

Conversion (*c*) of (*R*,*S*)-CPOMe was calculated as follows:

$$c = \frac{([S]+[R])V}{n_{\mathrm{CPME},0}} \times 100\% \quad (2)$$

The enantioselectivity was calculated by the following Eq. (3).

$$\mathrm{E} = \frac{\ln[1-c(1+ee_P)]}{\ln[1-c(1-ee_P)]} \quad (3)$$

where, [*S*] and [*R*] are the concentrations of (*S*)-CP and (*R*)-CP in reaction mixture, respectively; *V* represents the volume of the reaction mixture; $n_{CPME,0}$ is initial amount of (*R*,*S*)-CPOMe (mmol).

Synthesis of (*R*, *S*)-CPOMe

(*R*, *S*)-CPOMe was synthesized with commercially available (*R*, *S*)-CP (purity, 98%) by esterification reaction. (*R*, *S*)-CP (17.4 mmol, 5.0 g) was dissolved in excess methanol (0.17 L), then 3% (w/v) sulfuric acid was added as catalyst. This reaction was performed in an oil bath at 70 °C for 6 hours. The reaction keep monitoring with TLC plate until the esterification reaction was terminated for six hours. The saturated sodium bicarbonate solution was used to wash reactive mixture, which was precipitated as a solid by washing with deionized water to neutral. The precipitated solid was recrystallized once by methanol and deionized water, and the mixture was filtered and the resulting solid was dried in oven. Finally, (*R*, *S*)-CPOMe was obtained. The yield was greater than 86%, and the purity of (*R*, *S*)-CPOMe was higher than 98% determined by HPLC.

Lipase-catalyzed Hydrolysis of (*R*, *S*)-CPOMe

The lipase-catalyzed hydrolysis reaction was operated in a 25 mL schlenk tube. A certain amount of (*R*, *S*)-CPOMe and lipase were added to 1 mL of 0.1 mol/L sodium phosphate buffer containing *β*-CDs to initialize the reaction. The agitation speed was kept at 600 rpm. Figure 1 show lipase-catalyzed hydrolysis reaction. After the termination of the reaction, 1-2 mL of acetonitrile was added to the suspension, which dissolved all insoluble substrates and products. Then, the reaction solution was filtered via a 0.45 μm microporous membrane, and product concentration was determined by HPLC. In this paper, all experiments were repeated three times under same conditions and the accuracy of the duplicate values was within ± 3%.

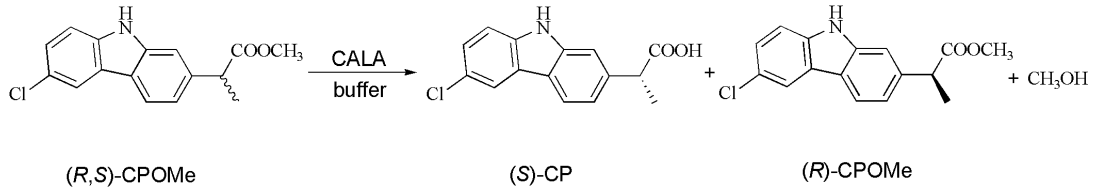

Figure 1. Lipase catalyzed hydrolysis of (*R*,*S*)-CPOMe in buffer median.

Design of Experiments and Statistical Analysis

RSM was employed to predict the process of hydrolysis of (*R*,*S*)-CPOMe by enzyme catalyzed in a phosphate buffer solution. The effect of important factors on *c* and ee_p were investigated, including temperature (A), pH (B), lipase concentration (C), cyclodextrin concentration (D), substrate loading (E) and reaction time (F). In RSM equations, parameters were acquired by regression analysis of the experimental data.

The independent variables were reaction temperature (A, 40-100 °C), pH (B, 4-9), lipase concentration (C, 10-50 mg/mL), HE-*β*-CD concentration (D, 0-50 mmol/L), substrate loading (E, 0.01-0.06 mmol) and reaction time (F, 2-36 h). It is found that the quadratic model of response surface for optimization is suitable and effective by experimental data analysis. The second-order polynomial equations for *c* and ee_p are shown in Eqs. (4) and (5).

$$c = \alpha_0 + \sum_{i=1}^{k} \alpha_i x_i + \sum_{i=1} \sum_{j=i+1}^{k} \alpha_{ij} x_i x_j + \sum_{i=1}^{k} \alpha_{ii} x_i^2 \quad (4)$$

$$ee_p = b_0 + \sum_{i=1}^{k} b_i x_i + \sum_{i=1} \sum_{j=i+1}^{k} b_{ij} x_i x_j + \sum_{i=1}^{k} b_{ii} x_i^2 \quad (5)$$

where, *c* and ee_p represent conversion and enantiomeric excess, respectively; α_0 and b_0 are the constant coefficient; α_i and b_i, α_{ij} and b_{ij}, α_{ii} and b_{ii} are the linear coefficient, squared coefficient, and cross-product coefficient, respectively; *k* is the number of factors; x_i and x_j are the independent variable. All the coefficients in Eqs. (4) and (5)

were calculated by analysis of variance (ANVOVA). Design Expert (version 8.0.5b) can be employed to acquire all coefficient of model and, optimize multiple responses.

RESULT AND DISCUSSION

Selection of various Enzymes

Stereoselective hydrolysis of (*R*,*S*)-CPOMe enantiomers was carried out through enzymatic in aqueous medium. Different enzymes show various selectivity and catalytic activity. Herein, the effect of nine enzymes on conversion and enantiomeric excess were investigated for stereoselective hydrolysis of (*R*,*S*)-CPOMe (Table 1). Among them, CALA, Lipase AY, Lipase AK as well as Lipase PS were able to be dissolved in the buffer solution, while other enzymes were insoluble or slightly soluble. Soluble enzymes increase the substrate contact with the enzyme to enhance the rate of hydrolysis. The results show the highest E of 30.48 is obtained with CALA. When the catalyst is CALA, the total conversion and product purity are relatively high, which can reach up to 19.90% and 92.12%, respectively. Compared with other lipases, CALA has stronger association with the oil-water interface to expose the active site, so that the binding ability between substrate and lipase becomes stronger. Meanwhile, high interfacial activation can increase the hydrophobicity of the catalytic site, leading to reorientation of the α-helix, thereby exposing the active site to enhance catalytic activity. Therefore, CALA is chosen as the optimal catalyst for further experiments.

Table 1. Results of hydrolysis of (*R*,*S*)-CPOMe catalyzed by different lipases

lipase	source	ee_p (%)	*c* (%)	E
CALA	*Candida antarctica A*	92.12 ± 0.08	19.90 ± 0.35	30.48 ± 1.11
Novozym 435	*Candida antarctica B*	48.44 ± 0.24	4.30 ± 2.32	2.94 ± 0.37
Lipase AY	*Candida rugosa*	--	--	--

Lipase PS	*Burkholderia cepacia*	89.02 ± 0.17	0.05 ± 3.00	17.22 ± 1.56
Lipase AK	*Pseudomonas*	--	--	--
Novozym40086	*Aspergillus oryzae*	86.92 ± 0.20	0.45 ± 2.55	14.35 ± 1.62
Lipozyme RM	*Rhizomucor miehei*	91.18 ± 0.11	0.45 ± 0.32	21.77 ± 0.94
Lipozyme TL	*Candida cylindracea*	--	--	--
PPL	*Porcine pancreatic*	--	--	--

Conditions: 20 mg/mL lipase, 0.02 mmol (*R*,*S*)-CPOMe, reaction temperature 40 °C, pH 6.0, and reaction volume 1 mL.

Selection of Additive Types

As shown in Table 1, with CALA as the biocatalyst, high enantioselectivity is achieved, while the total conversion of (*R*,*S*)-CPOMe is relatively low. Therefore, it is necessary to improve the substrate conversion. The solubility of (*R*,*S*)-CPOMe in aqueous solution is very poor. Low solubility of ester will result in low total conversion in enzymatic hydrolysis reaction system[30,31]. Adding the additives into aqueous phase can improve the solubility of substrate and the hydrolysis reaction rate [32,33].

Nine additives are employed to improve stereoselective hydrolysis of (*R*,*S*)-CPOMe (Table 2). The ee_P is slightly enhanced with additive added. It is satisfied that the total conversion and enantioselectivity are greatly increased by the addition of Tween 80, HP-*β*-CD, Me-*β*-CD and HE-*β*-CD. This may be because tween 80 acts as an emulsifier to enhance the solubility of the insoluble substrate, thereby increasing the rate of hydrolysis reaction. *β*-CD derivative has a special chemical structure with an internal hydrophobic cavity and external hydrophilic surface. Hydrophilic *β*-CD derivative and CPOMe can form a water-soluble inclusion complex, which can enhance the dissolution of the substrate. Meanwhile, *β*-CD

derivatives as chiral additives can selectively identify (*R*) and (*S*)-enantiomers. The selectivity is enhanced by the synergistic effect of CALA and *β*-CD derivatives. Meanwhile, HE-*β*-CD is considered as an excellent solubilizer because it is pollution-free, not toxic, economical and easy to be separated from products. The total conversion rate with the addition of tween 80 was increased by 5% compared with that of HE-*β*-CD, while the enantioselectivity was relatively low. What's more, tween 80 as surfactant generally would cause a complex purification process and high production cost. Thus, HE-*β*-CD is chosen as the optimal additive for enzymatic hydrolysis of (*R,S*)-CPOMe.

Table 2. Effects of different additives on lipase-catalyzed hydrolysis of (*R*,*S*)-CPOMe

Additives	ee_p **(%)**	*c* **(%)**	**E**
None	95.44 ± 0.08	11.12 ± 0.31	48.20 ± 1.85
Span 60	97.69 ± 0.06	15.27 ± 0.23	102.00 ± 2.87
Tween 60	97.34 ± 0.05	18.01 ± 0.45	91.67 ± 2.23
Tween 80	96.76 ± 0.05	35.47 ± 0.18	103.69 ± 1.61
Macrogol 400	97.93 ± 0.07	16.14 ± 0.43	114.94 ± 3.46
HP-*β*-CD	96.94 ± 0.09	27.26 ± 0.27	91.89 ± 3.26
SBE-*β*-CD	96.38 ± 0.06	10.48 ± 0.62	60.62 ± 1.91
Me-*β*-CD	97.36 ± 0.08	30.56 ± 0.20	114.08 ± 3.07
HE-*β*-CD	97.48 ± 0.05	30.89 ± 0.24	120.49 ± 2.17
CM-*β*-CD	95.92 ± 0.07	10.80 ± 0.69	53.83 ± 1.97

Conditions: 40 mg/mL CALA, 0.05 mmol (*R*,*S*)-CPOMe, 20 mmol/L additives, reaction temperature 80 °C, pH 6.0, reaction time 14 h, and reaction volume 1 mL.

Regression Model and Statistical Analysis

The effect of six independent variables, including temperature, CALA concentration, pH, HE-*β*-CD concentration, substrate loading and reaction time on resolution performance were investigated. The *c* and ee_p of different experiment conditions are listed in Table 3.

Table 3. Central composite design matrix of the independent variables with their corresponding response

run	Temperature (°C)	pH	CALA (mg/mL)	HE-*β*-CD (mmol/L)	Substrate ($\times 10^{-3}$ mmol)	Reaction time (h)	*c* (%)	ee_p (%)
1	40	6	20	0	20	4	3.8	75.78
2	50	6	20	0	20	4	5.7	85.72
3	60	6	20	0	20	4	10.59	90.04
10	80	5	20	0	20	4	13.26	91.68
11	80	5.5	20	0	20	4	15.29	92.76
21	80	6.5	40	0	20	4	19.74	95.06
22	80	6.5	45	0	20	4	18.28	94.42
23	80	6.5	40	0	50	4	10.68	93.9
24	80	6.5	40	5	50	4	14.31	94.23
38	80	6.5	40	40	40	30	46.17	95.94
39	80	6.5	40	40	45	30	46.26	96.02
40	80	6.5	40	40	50	30	46.07	95.92
41	80	6.5	40	40	60	30	39.91	95.67
42	80	6.5	40	40	50	6	31.57	95.5
43	80	6.5	40	40	50	12	38.53	95.64
44	80	6.5	40	40	50	19	42.09	95.22
45	80	6.5	40	40	50	24	43.95	95.08
46	80	6.5	40	40	50	30	46.07	95.94
47	80	6.5	40	40	50	36	46.27	95.09
4	70	6	20	0	20	4	13.03	92.59
6	80	6	20	0	20	4	16.56	94.16
7	90	6	20	0	20	4	7.31	91.3
8	100	6	20	0	20	4	1.25	87.7
9	80	4	20	0	20	4	4.8	88.5
14	80	7	20	0	20	4	15.67	92.79
15	80	9	20	0	20	4	2.3	73.8
16	80	6.5	15	0	20	4	9.07	93.8
17	80	6.5	20	0	20	4	12.52	94.47
18	80	6.5	25	0	20	4	15.34	94.56
33	80	6.5	40	40	15	30	47.4	87.1
34	80	6.5	40	40	20	30	46.9	91.5
35	80	6.5	40	40	25	30	46.42	94.02
36	80	6.5	40	40	30	30	46.25	95.08
37	80	6.5	40	40	35	30	46.58	95.78

25	80	6.5	40	10	50	4	18.57	94.58
26	80	6.5	40	15	50	4	22.22	95.34
27	80	6.5	40	20	50	4	25.76	95.42
28	80	6.5	40	25	50	4	24.21	95.52
29	80	6.5	40	30	50	4	26.74	95.88
30	80	6.5	40	35	50	4	29.11	95.92
31	80	6.5	40	40	50	4	26.19	95.94
32	80	6.5	40	40	10	30	48.2	83.16
12	80	6	20	0	20	4	16.66	94.16
13	80	6.5	20	0	20	4	17.6	94.55
19	80	6.5	30	0	20	4	16.03	95.14
20	80	6.5	35	0	20	4	17.45	93.94

To obtain the coefficients, the experimental data was employed to fit both Eqs. (4) and (5) polynomial equation. The multiple quadratic regression models for ee_p and c could be expressed by the following second order polynomial Eqs. (6) and (7).

$$c(\%) = 42.50+6.2A-1.69B+4.62C+6.24D-3.83E+9.44F+2.91DE \\ -18.46A^2-9.99B^2-4.9C^2-7.55D^2-2.36E^2-6.79F^2 \quad (6)$$

$$ee_P(\%) = 94.35+11.27A-6.36B+1.12C-1.33D+2.71E+0.31F+3.45DE \\ -16.08A^2-12.72B^2-0.94C^2-1.14D^2-6.57E^2+0.13F^2 \quad (7)$$

When p-value is more than 0.0500, it implies that the model coefficients are insignificant. The p-value of c and ee_p models are less than 0.0001, indicating two models are significant (Table 4). The corresponding correlation coefficients R^2 of c and ee_p are 0.9884 and 0.9745, respectively, indicating that the model has high reliability and fitting well with the experimental data.

Table 4. ANOVA for response surface reduced quadratic model

	c					***ee*$_p$**			
source	**mean square**	***F* value**	***p*-value Prob > **		**source**	**mean square**	***F* value**	***p*-value Prob >**	
Model	830.47	216.52	< 0.0001	significant	Model	79.71	97.17	< 0.0001	significant
α_A	89.28	23.28	< 0.0001		b_A	295.01	359.61	< 0.0001	
α_B	7.25	1.89	0.1786		b_B	102.55	125.01	< 0.0001	

α_C	56.14	14.64	0.0006	b_C	3.33	4.06	0.0522
α_D	62.72	16.35	0.0003	b_D	2.85	3.48	0.0711
α_E	85.91	22.40	< 0.0001	b_E	42.83	52.21	< 0.0001
α_F	431.57	112.52	< 0.0001	b_F	0.47	0.57	0.4567
α_{AB}	--	--	--	b_{AB}	--	--	--
α_{AC}	--	--	--	b_{AC}	--	--	--
α_{AD}	--	--	--	b_{AD}	--	--	--
α_{AE}	--	--	--	b_{AE}	--	--	--
α_{AF}	--	--	--	b_{AF}	--	--	--
α_{BC}	--	--	--	b_{BC}	--	--	--
α_{BD}	--	--	--	b_{BD}	--	--	--
α_{BE}	--	--	--	b_{BE}	--	--	--
α_{BF}	--	--	--	b_{BF}	--	--	--
α_{CD}	--	--	--	b_{CD}	--	--	--
α_{CE}	--	--	--	b_{CE}	--	--	--
α_{CF}	--	--	--	b_{CF}	--	--	--
α_{DE}	25.15	6.56	0.0152	b_{DE}	35.21	42.93	< 0.0001
α_{DF}	--	--	--	b_{DF}	--	--	--
α_{EF}	--	--	--	b_{EF}	--	--	--
α_{AA}	267.56	69.76	< 0.0001	b_{AA}	202.96	247.41	< 0.0001
α_{BB}	164.8	42.97	< 0.0001	b_{BB}	267.19	325.71	< 0.0001
α_{CC}	7.89	2.06	0.161	b_{CC}	0.29	0.36	0.5542
a_{DD}	32.95	8.59	0.0061	b_{DD}	0.75	0.91	0.3467
α_{EE}	7.2	1.88	0.1798	b_{EE}	56.1	68.39	< 0.0001
α_{FF}	41.48	10.82	0.0024	b_{FF}	0.016	0.02	0.8895

Influence of Reaction Temperature and pH

It is well known that enzymes are proteins with biocatalytic activity, whose activity is usually affected by temperature. The reaction rate will be reduced if temperature is too low. However, excess temperature result in the irreversible protein denaturation of enzyme and the decrease of enzymatic activity. Therefore, a suitable temperature should be selected for enzymatic hydrolysis reaction. In addition, the enzyme contains both amino and carboxyl groups, which have effect on the activity of

enzyme owning to pH of solution. According to the experimental results, RSM model is used to simulate the above influence. As shown in Figure 2, the effect of temperature and pH on *c* and ee_p is similar. From Figure 2a, the *c* increases firstly as temperature increases, then reaches a maximum at 76 °C. The *c* is decreased with the further increase of temperature (≥ 76 °C). This result shows that CALA is a heat-resistant lipase with good temperature tolerance, benefiting for catalytic reaction at a high temperature[34,35]. Likewise, the CALA has the optimal pH of 6.0. From Figure 2b, the maximum of ee_p is observed at temperature of 76 °C and pH of 6.0. In order to obtain high *c* and ee_p, the reaction temperature and pH are set at 76 °C and 6.0, respectively.

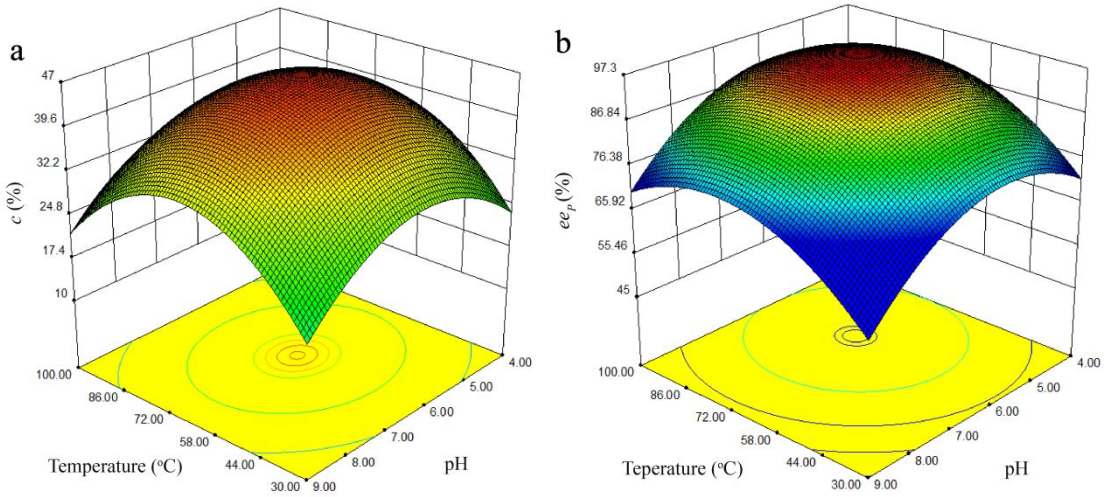

Figure 2. Effects of reaction temperature and pH on *c* and ee_p. Conditions: 40 mg/mL CALA, 0.05 mmol (*R*, *S*)-CPOMe, 35 mmol/L HE-*β*-CD, and reaction time 30 h.

Influence of Concentration of CALA and the Loading of Substrate

Influence of the concentration of CALA and the loading of substrate on *c* and ee_p was investigated, fixing the total volume of 1 mL (Figure 3). As shown in Figure 3a, with the concentration of CALA increase, the *c* value increases rapidly (≤ 40 mg/mL) and decrease slightly (≥ 40 mg/mL). However, the *c* increases slowly with the increase of the substrate loading before 0.02 mmol, then decreases dramatically

with further increase. From Figure 3b, the ee_p is slightly increased by increasing the concentration of CALA, while increasing substrate loading can greatly influence the ee_p. With the increase of substrate loading, the ee_p increases, then reaches maximum at about 0.05 mmol (*R*, *S*)-CPOMe. With substrate loading further increase, ee_p decrease. To acquire higher product purity and yield, the concentration of CALA should be kept being 40 mg/mL.

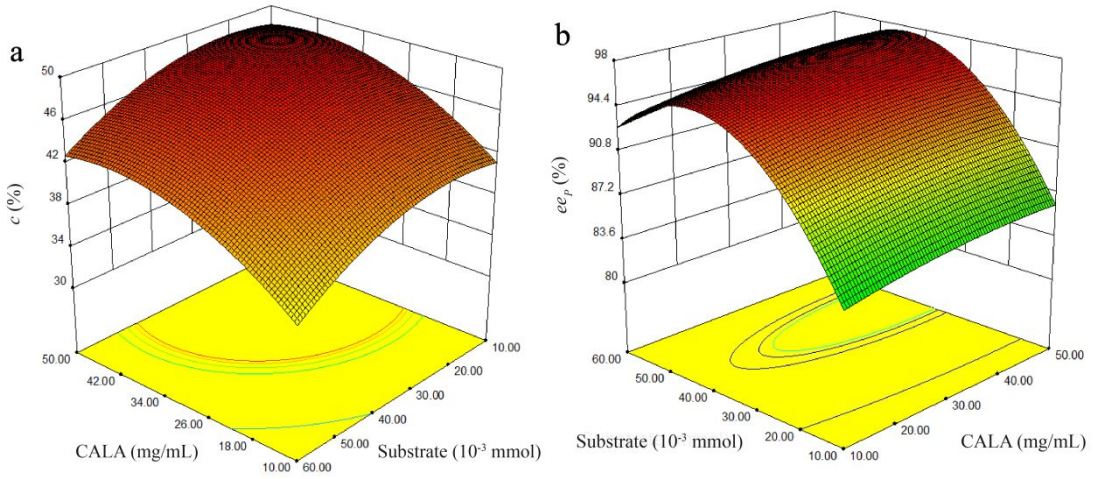

Figure 3. Effects of the loading of substrate and the concentration of CALA on *c* and ee_p. Conditions: 35 mmol/L HE-*β*-CD, reaction temperature 76 °C, pH 6.0, and reaction time 30 h.

Influence of pH and HE-*β*-CD Concentration

With the addition of HE-*β*-CD, *c* can be obviously increased while ee_p is not affected. In addition, pH may affect the dissociation of hydroxyl groups in HE-*β*-CD, resulting in changes in the existing form of HE-*β*-CD. Therefore, the effects of pH and HE-*β*-CD concentration on *c* and ee_p are necessary to be studied. From Figure 4, as the concentration of HE-*β*-CD increases, the *c* can be greatly enhanced. Increasing HE-*β*-CD concentration at any tested pH, *c* increases fastly, and then increases slowly when HE-*β*-CD concentration is above 35 mmol/L. Meawhile, there is slightly influence of HE-*β*-CD concentration on ee_p. However, in any HE-β-CD concentration,

both c and ee_p rise rapidly with increasing pH, reaching maximum at pH around 6.0. Continuing to increase the pH, c and ee_p obviously reduced, which is consistent with the above trend (Figure 2). The β-CD derivatives are able to include hydrophobic molecules inside their cavity to form inclusion complexes that are soluble in water [36]. Meanwhile, the inclusion equilibrium constants between HE-β-CD and the reactant (CPOMe) is evaluated as 11937.85 L/mol by using phase solubility method (Figure S1), which indicates that HE-β-CD has a stronger inclusion ability for (*S*)-CPOMe than that for (*R*)-CPOMe. The concentration of fast-reaction enantiomer in water was increased by adding β-CD derivatives, which led to the increase of enantioselectivity. To achieve high c and ee_p, 35 mmol/L HE-β-CD and pH 6.0 are selected.

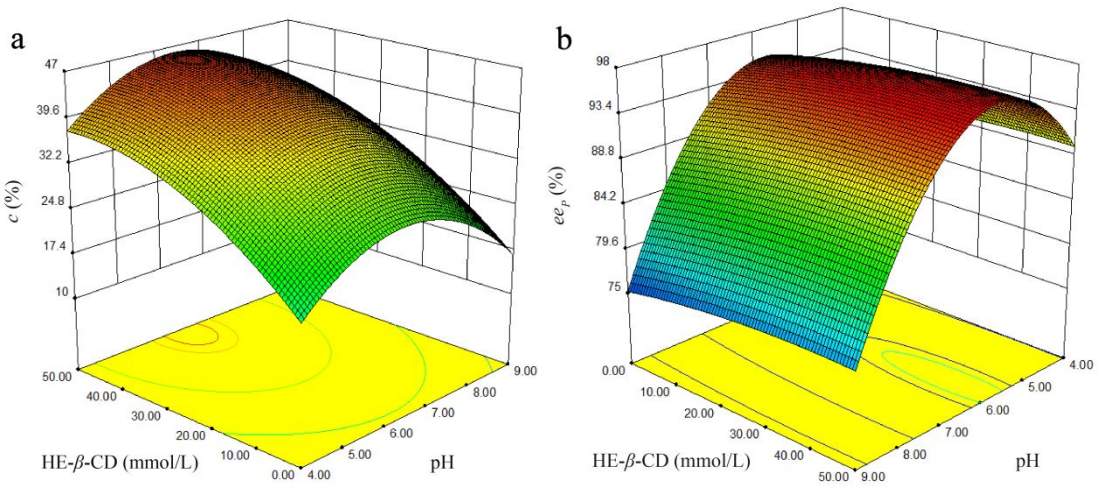

Figure 4. The effects of pH and HE-β-CD concentration on c and ee_p. Conditions: 40 mg/mL CALA, 0.05 mmol (*R*, *S*)-CPOMe, temperature 76 °C, and reaction time 30 h.

Influence of HE-β-CD Concentration and Substrate Loading

By adding HE-β-CD, the substrate conversion can be improved, which is accustomed to the inclusion interaction between HE-β-CD and the substrate. Therefore, the effect of HE-β-CD concentration and substrate loading on c and ee_p is necessary to be investigated. As shown in Figure 5, the trend of the influence of substrate loading on c and ee_p is the same as that in Figure 3. And it is also observed

that the effect of HE-β-CD concentration on c and ee_p is consistent with the trends of Figure 4. It can be concluded that 35 mmol/L HE-β-CD and 0.05 mmol (*R*,*S*)-CPOMe are preferential to achieve high c and ee_p in the reaction system.

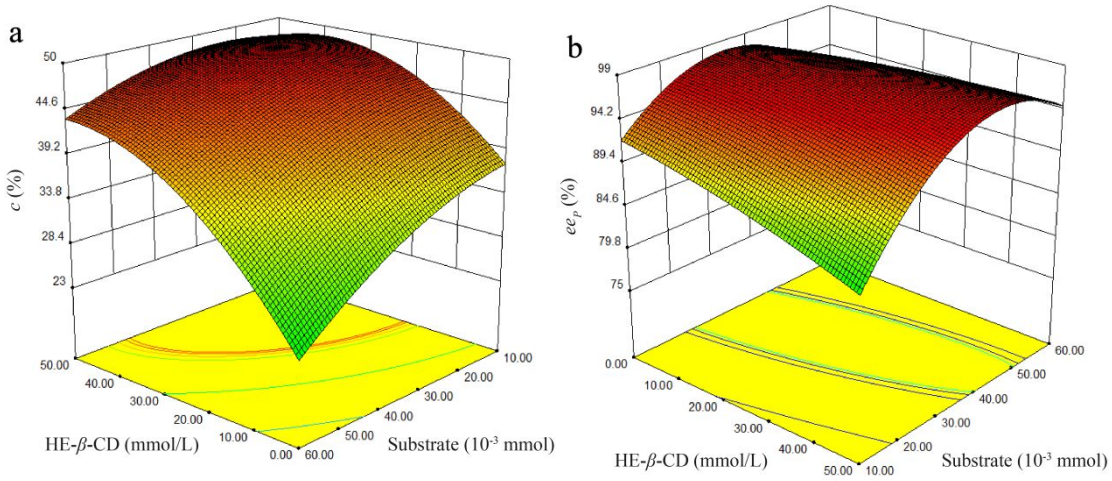

Figure 5. Effects of the loading of substrate and HE-β-CD concentration on c and ee_p. Conditions: 40 mg/mL CALA, temperature 76 °C, pH 6.0, and reaction time 30 h.

Influence of Temperature and Reaction Time

Temperature has an important influence on enzymatic activity. The rate of the enzymatic hydrolysis is affected by temperature, thereby changing the time of the entire reaction. Thus, the relationships among temperature, reaction time, c as well as ee_p were studied (Figure 6). From Figure 6, c and ee_p increase significantly as the temperature increases (≤ 76 °C), and they reduced sharply with temperature further increased (≥ 76 °C). The maximum of c and ee_p can be reached at 76 °C, The trends is coincided with the effect of temperature in Figure 2. There is a rapid increase of c when reaction time is before 30 h and then a slow increase is observed. It is obvious that c increases greatly with reaction time increases, c increases slowly after 30 h. However, there is nearly no influence of reaction time on ee_p. Therefore, 30 h is enough to obtain large conversion and high product purity.

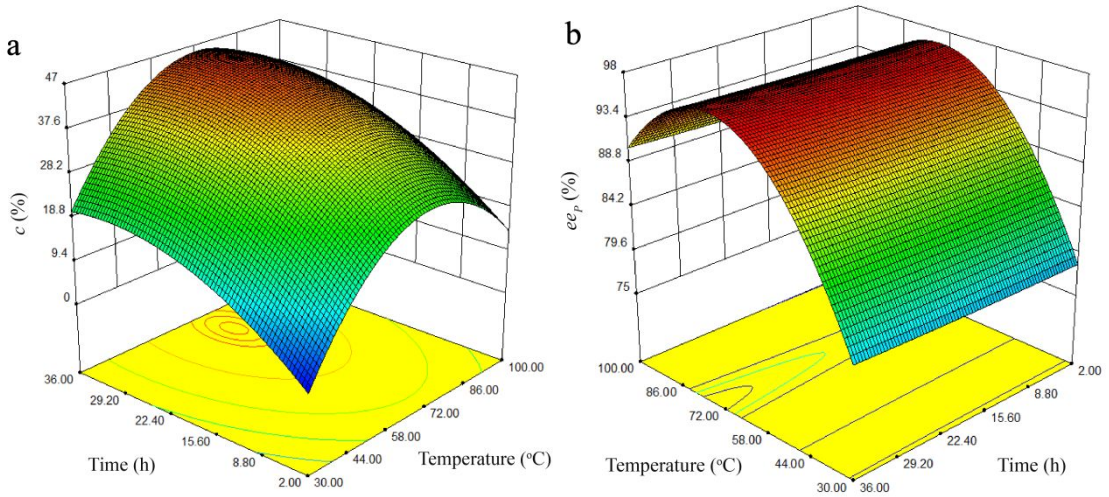

Figure 6. Effects of reaction temperature and time on conversion c and ee_p, Conditions: 40 mg/mL CALA, 0.05 mmol (*R*, *S*)-CPOMe, 35 mmol/L HE-β-CD, and pH 6.0.

APPLICATION AND VALIDATION OF THE MODEL

The optimal reaction conditions can be obtained according to the above results, including pH 6.0, 40 mg/mL CALA, 0.05 mmol substrate, 35 mmol/L HE-β-CD, 76 °C for temperature, and 30 h for reaction time. The enzymatic hydrolysis reaction was repeated three times under optimal conditions. Product purity was analyzed through HPLC (Figure 7). The chromatograms of racemic CP and the product are shown in Figure 7a and b, respectively. The experimental results and predicted values of RSM under the optimal conditions are displayed in Table 5. Relative deviation indicates that the experimental values are coincided with the model prediction very well. Therefore, the lipase-catalyzed hydrolysis process can be simulated and optimized to obtain optimal process parameters through the RSM. The results can provide the theoretical basis for process design and operation of large-scale production. However, more factors, such as reactor type and size, economic benefits and safety, should be considered in applying these process parameters to industrial-scale production.

Table 5. Predicted and observed values for the response variables based on optimal conditions.

Response variable	Predicted value	Experimental value	Relative deviation
c (i)	45.76%	46.07%	0.68%
ee_p (i)	97.02%	96.24%	0.80%
c (ii)	44.68%	43.86%	1.84%
ee_p (ii)	96.87%	95.38%	1.54%
c (iii)	44.43%	42.91%	3.42%
ee_p (iii)	92.36%	94.34%	2.14%

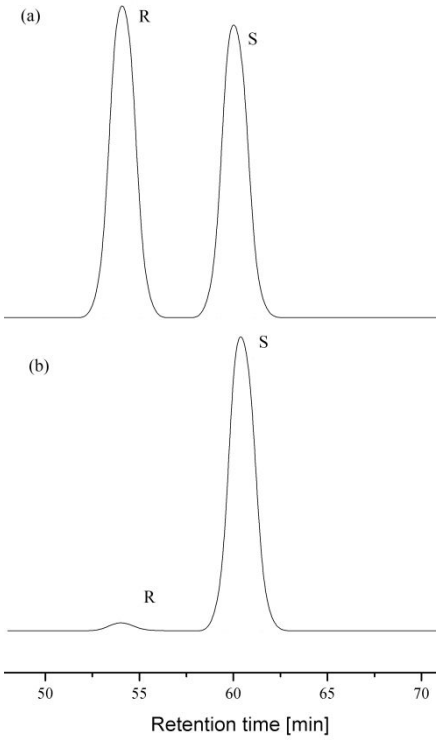

Figure 7. Chromatograms of (*R*, *S*)-CP and product by HPLC. (a) CP sample (racemic), (b) product of lipase catalyzed stereoselective hydrolysis (*R*,*S*)-CPOMe.

CONCLUSION

In this paper, an efficient reaction system of stereoselective resolution of (*R*, *S*)-CPOMe by lipase-catalyzed hydrolysis was constructed to obtain (*S*)-CP. *Candida antarctica* lipase A was selected as the most efficient catalyst. With the addition of HE-*β*-CD into the reaction system, *c* was increased from 11.12% to 30.84%, while ee_P value was changed slightly. The RSM model was applied to simulate and optimize the reaction system to acquire the optimal reaction conditions. The results show that ee_P depends primarily on temperature, pH and substrate loading. Other conditions such as HE-*β*-CD concentration and time, have small effect on ee_P, but have great influence on substrate conversion. Experimental results show that ee_p and *c* under the optimal reaction conditions can reach 96.24% and 46.07%, respectively. These results are coincided well with the model predicted values, which shows that the RSM of quadratic model was a powerful tool to optimize the lipase-catalyzed hydrolysis of (*R*, *S*)-CPOMe process. This work provide important guiding significance for the large-scale production.

ASSOCIATED CONTENT

Supporting Information

Phase solubility diagram of CPOMe in presence of HE-*β*-CD (Figure S1).

AUTHOR INFORMATION

* Corresponding author.

E-mail address: tangkewen@sina.com (K.W. Tang).

Tel.: +86 13762003936 Fax: +86 730 8640921

E-mail address: qpanny@163.com (P.L. Zhang).

Tel.: +86 13786023146 Fax: +86 730 8640921

Notes

The authors declare no competing financial interest.

ACKNOWLEDGMENT

This work was supported by the National Natural Science Foundation of China (grant number. 21676077).

REFERENS

1. Simonyi, M. On Chiral Drug Action. Med. Res. Rev. **2010**, 4, 359-413.

2. Drayer, D. E. Pharmacodynamic and Pharmacokinetic Differences Between Drug Enantiomers in Humans: An overview. *Clin. Pharmacol. Ther.* **1986**, *40*, 125-33.

3. Rekoske, J. E. Chiral Separations. *AICHE J.* **2001**, *47*, 2-5.

4. Sheldon, R. Chirotechnology: Industrial Synthesis of Optically Active Compounds. Angew. *Chem. Int. Ed.* **1994**, *106*, 1466–1467.

5. Chen, D. M.; Fu, Q.; Li, N. Enantiomeric Separation of Naproxen by High Performance Liquid Chromatography using CHIRALCEL OD as Stationary Phase. *Chin. J. Anal. Chem*. **2007**, *35*,75-78.

6. Rouhi, A. M. Chiral Business. *Chem. Eng. News.* **2003**, *81*, 45-45.

7. Kim, D.; Ha, M. W.; Hong, S.; et al. Enantioselective Synthesis of Chiral α-Azido and α-Aryloxy Quaternary Stereogenic Centers via the Phase-Transfer-Catalyzed α-Alkylation of α-Bromomalonates, Followed by SN2 Substitutio. *J. Org. Chem.* **2017**, *82*, 4936-4943.

8. Liu, G. Y.; Zhang, P. L.; Xu, W. F.; et al. Lipase-Catalyzed Hydrolysis of (+,-)-2-(4-Methylphenyl)propionic Methyl Ester Enhanced by Hydroxypropyl-β-Cyclodextrin. *J. Chem. Technol. Biotechnol.* **2019**, *94*, 147-158.

9. Simon, M.; Donnellan, P.; Glennon, B.; et al. Resolution Via Diastereomeric Salt Crystallization of Ibuprofen Lysine: Binary and Ternary Phase Diagram Studies. *Chem. Eng. Technol.* **2018**, *41*,921-927.

10. O'Brien, A. G.; Horváth, Z.; Lévesque, F. Continuous Synthesis and Purification by Direct Coupling of a Flow Reactor with Simulated Moving-Bed Chromatography. *Angew. Chem. Int. Ed.* **2012**, *51*, 7028-7030.

11. San Román, M. F.; Bringas, E.; Ibanez, R. Liquid Membrane Technology: Fundamentals and Review of its Applications. *J. Chem. Technol. Biotechnol.* **2010**, *85*, 2-10.

12. Tang, K. W.; Zhang, H.; Liu, Y. Experimental and Simulation on Enantioselective Extraction in Centrifugal Contactor Separators. *AICHE J.* **2013**, *59*, 2594-2602.

13. Holbach, A.; Godde, J.; Mahendrarajah, R.; Kockmann, N. Enantioseparation of Chiral Aromatic Acids in Process Intensified Liquid–Liquid Extraction Columns. *AIChE J.* **2015**, *6*1, 266-276.

14. Tang, K. W.; Zhang, P. L.; Pan, C. Equilibrium Studies on Enantioselective Extraction of Oxybutynin Enantiomers by Hydrophilic β-Cyclodextrin Derivatives. *AIChE J.* **2011**, *57*, 3027-3036.

15. Lv, C. G.; Jia, G. F.; Zhu, W. T. Enantiomeric Resolution of New Triazole Compounds by High-performance Liquid Chromatography. *J. Sep. Sci*. **2015**, *30*, 344-351.

16. Sunsandee, N.; Ramakul, P.; Pancharoen, U. Enantioseparation of (S)-Amlodipine from Pharmaceutical Industry Wastewater by Stripping Phase Recovery via HFSLM: Polarity of Diluent and Membrane Stability Investigation. *Sep. Purif. Technol.* **2013**, *116*, 405-414.

17. Karadeniz, F.; Bayraktar, E.; Mehmetoglu, U. Kinetic Resolution of Racemic 1-Phenyl-1-propanol by Lipase Catalyzed Enantioselective Esterification Reaction. *Artif. Cell. Blood. Sub.* **2010**, *38*, 288–293.

18. Siodmiak, T.; Mangelings, D.; Heyden, Y. V. High Enantioselective Novozym 435-Catalyzed Esterification of (R,S)-Flurbiprofen Monitored with a Chiral Stationary Phase. *Appl. Biochem. Biotech.* **2015**, *175*, 2769-2785.

19. Agustian, J.; Kamaruddin, A. H. The Reaction Mechanism and Kinetics Data of Racemic Atenolol Kinetic Resolution via Enzymatic Transesterification Process using Free Pseudomonas Fluorescence Lipase. *Int. J. Chem. Kinet.* **2016**, *48*, 253–265

20. Zhang, J.; Li, Y.; Qian, W.; et al. Lipase-catalyzed Enantioselective Transesterification of 3-Hydroxy-3-(2-thienyl) Propanenitrile in Liquid Carbon Dioxide. *Green Chem. Lett. Rev.* **2018**, *11*, 224-229.

21. Long, W. S.; Kamaruddin, A. H.; Bhatia, S. Enzyme Kinetics of Kinetic Resolution of Racemic Ibuprofen Ester using Enzymatic Membrane Reactor. *Chem. Eng. Sci.* **2005**, *60*, 4957–4970.

22. Chen, J.; Chiahui, W. U.; Wang, P. Kinetic and Thermodynamic Investigation of Lipase-Catalyzed Hydrolysis of (R,S)-3-Phenylbutyl Azolides. *Ind. Eng. Chem. Res.* **2012**, *51*, 3580-3586.

23. Zhang, Y. Y.; Liu, J. H. Kinetic Study of Enantioselective Hydrolysis of (R,S)-Ketoprofen Ethyl Ester using Immobilized T. Laibacchii Lipase. *Biochem. Eng. J.* **2011**, *4*, 40-46.

24. Hu, C.; Wang, N.; Zhang, W. Immobilization of Aspergillus Terreus Lipase in Self-assembled Hollow Nanospheres for Enantioselective Hydrolysis of Ketoprofen Vinyl Ester. *J. Biotechnol.* **2015**, *194*, 12–18.

25. Ye, J.; Yu, W.; Chen, G. Enantiomeric Separation of 2-Arylpropionic Acid Nonsteroidal Anti-Inflammatory Drugs by HPLC with Hydroxypropyl-β-Cyclodextrin as Chiral Mobile Phase Additive. *Biomed. Chromatogr.* **2010**, *24*, 799–807.

26. Chan, A. S. C. Asymmetric Catalytic Hydrogenation of α-Arylpropenoic Acids: U.S. Patent 5,202,474. 1993-4-13.

27. Yi, L.; Su, X.; Werth, P. Synthetic Processes of Carprofen: U.S. Patent Application 15/147,671. 2016-11-10.

28. Tang, K.; Song, L.; Liu, Y.; Miao, J. Enantioselective Partitioning of 2-Phenylpropionic Acid Enantiomers in a Biphasic Recognition Chiral Extraction System. *Chem. Eng. J.* **2012**, *180*, 293-298.

29. Yilmaz, E.; Sezgin, M.; Yilmaz, M. Immobilization of Candida Rugosa Lipase on Magnetic sol-gel Composite Supports for Enzymatic Resolution of (R,S)-Naproxen Methyl Ester. *J. Mol. Cata.l B: Enzyme.* **2011**, *69*, 35-41.

30. Kim, S. H.; Kim, T. K.; Shin, G. S. Enantioselective Hydrolysis of Insoluble (R,S)-Ketoprofen Ethyl Ester in Dispersed Aqueous Reaction System Induced by Chiral Cyclodextrin. *Biotechnol. Lett.* **2004**, *26*, 965–969.

31. Shin, G. S.; Lee, K. W.; Kim, T. K. Lipase-Catalyzed Production of Optically Active (S)-Flurbiprofen in Aqueous Phase Reaction System Containing Chiral Succinyl- β-Cyclodextrin. *J. Mol. Catal. B-Enzyme.* **2005**, *33*, 93–98.

32. Liu, G. Y.; Zhang, P. L.; Xu, F. W.; Tang, K. W. Lipase-Catalyzed Hydrolysis of (+,-)-2-(4-Methylphenyl) Propionic Methyl Ester Enhanced by Hydroxypropyl-β-Cyclodextrin. *J. Chem. Technol. Biotechnol.* **2019**, *94*, 147-158.

33. Eriksson, T.; Börjesson, J.; Tjerneld, F. Mechanism of Surfactant Effect in Enzymatic Hydrolysis of Lignocellulose. *Enzyme Microb. Technol.* **2002**, *31*, 353-364.

34. Kirk, O.; Christensen, M. W. Lipases from Candida a Ntarctica: Unique Biocatalysts from a Unique Origin. *Org. Process. Res. Dev.* **2002**, *6*, 446–451.

35. Suescun, A.; Rueda, N.; dos Santos, J. C. S.; Castillo, J. J.; Ortiz, C.; Torres, R.; Fernandez-Lafuente, R. Immobilization of Lipases on Glyoxyl–Octyl Supports: Improved Stability and Reactivation Strategies. *Process. Biochem.* **2015**, *50*, 1211–1217.

36. Bonnet, V.; Gervaise, C.; Favrelle, A.; et al. Enzymatic Catalysis in Presence of Cyclodextrins. *Curr. Org. Chem.* **2010**, *14*, 1323-1336.